SUPPLEMENTAL MATERIAL

Kubota et al., http://www.jem.org/cgi/content/full/jem.20081605/DC1

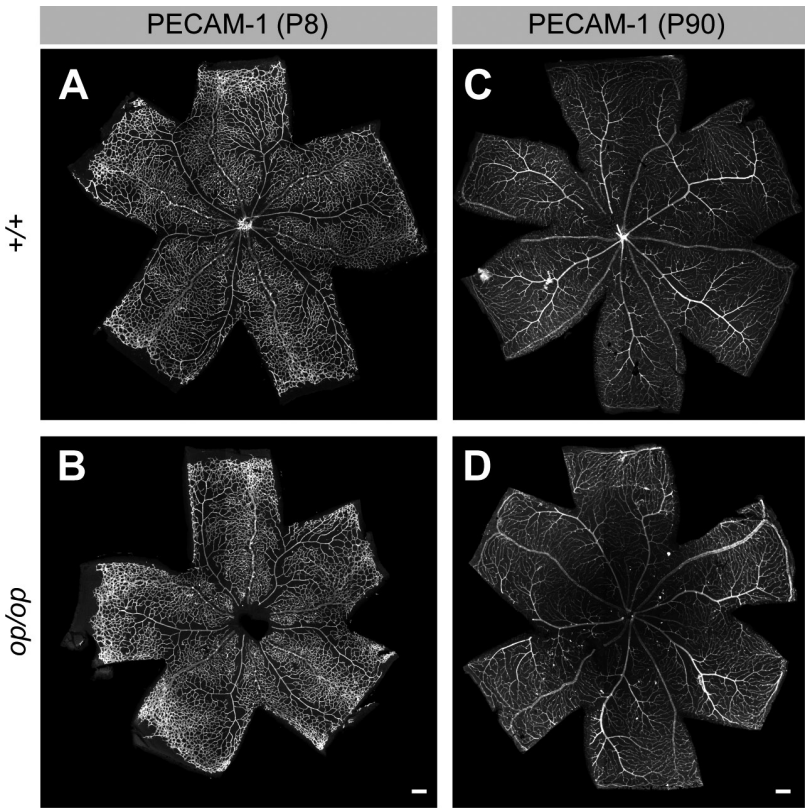

Figure S1. Vascular structure in *op/op* mice at P8 and P90. PECAM-1 staining at P8 or P90 (representative images of seven independent experiments). The reduced branching observed in *op/op* mice during the earlier stages of development became normal. Bars, 200 µm.

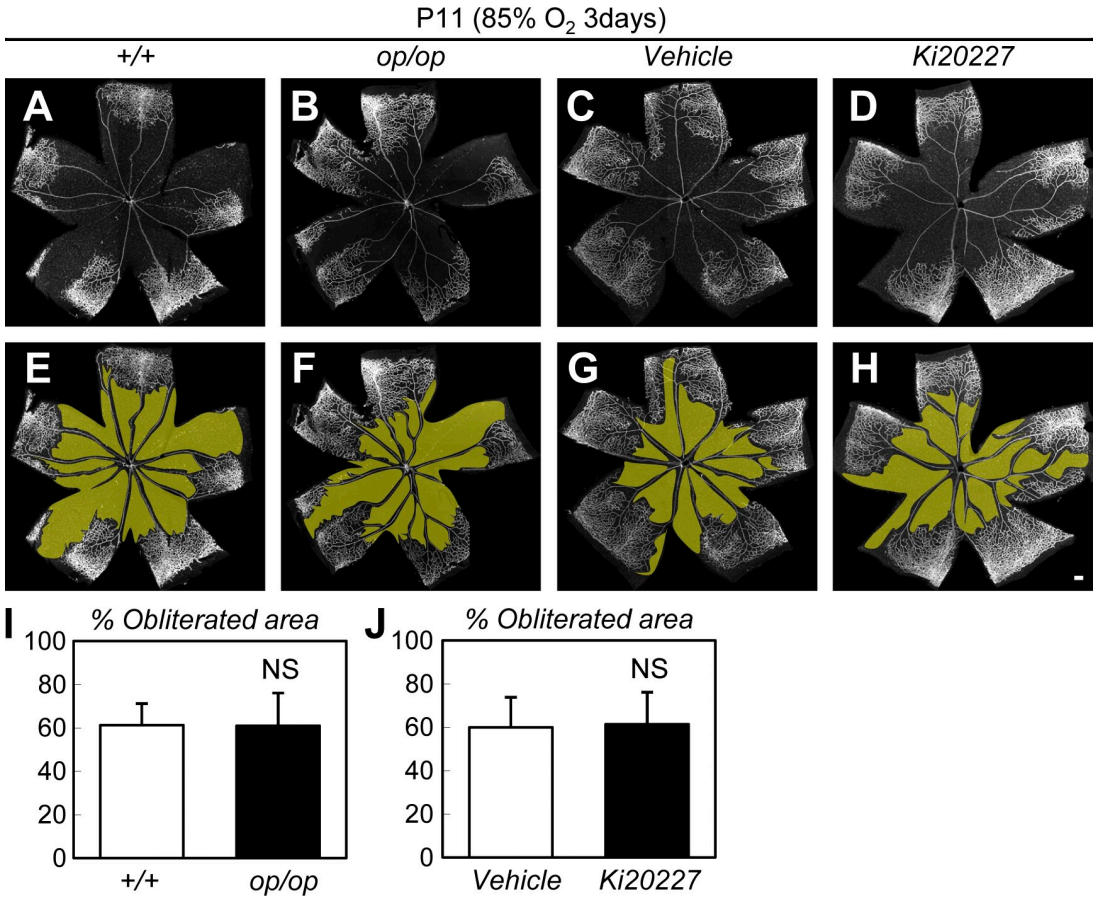

Figure S2. M-CSF deficiency or M-CSF inhibition does not affect vaso-obliteration in OIR model. (A–H) Isolectin staining of P11 retinas in an OIR model (representative images of five independent experiments). The yellow area in E–H indicates vaso-obliteration. Vascular resistance to hyper oxygen insults was not affected in *op/op* mice or in the presence of Ki20227. (I and J) Quantification (mean ± SD) of the vaso-obliterated area (i.e., quantification of the entire retina; n = 5). Bar, 200 µm.

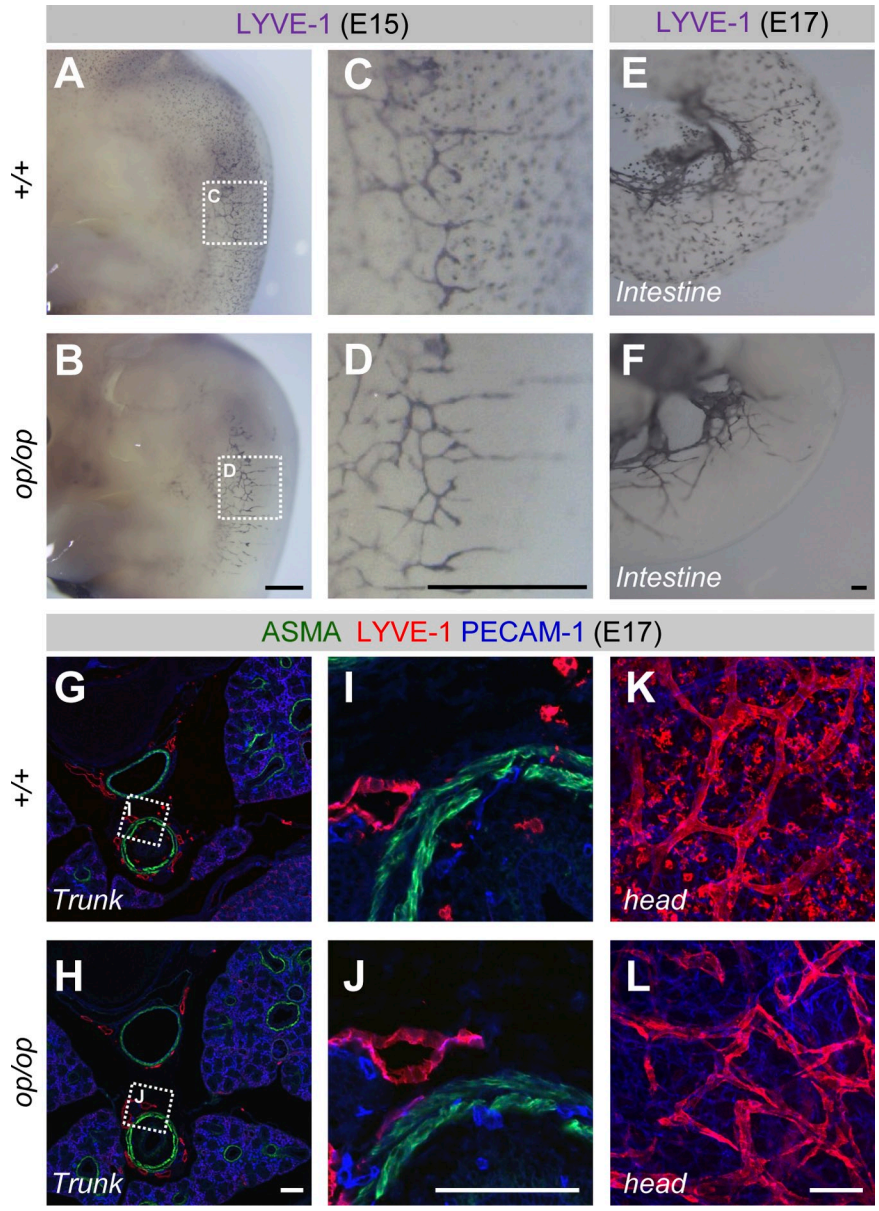

Figure S3. The *op/op* mice exhibited normal embryonic lymphangiogenesis but lacked LYVE-1⁺ macrophages. IHC with indicated antibodies in E15 embryos (A–D), the intestines harvested from E17 embryos (E and F), the areas of major trunk vessels in E17 embryonic sections (G–J), or the head skins in E17 embryos (K and L; representative images of three independent experiments). The *op/op* mice exhibited normal lymphatic branching, although they lacked LYVE-1⁺ macrophages. Bars, 100 μm.

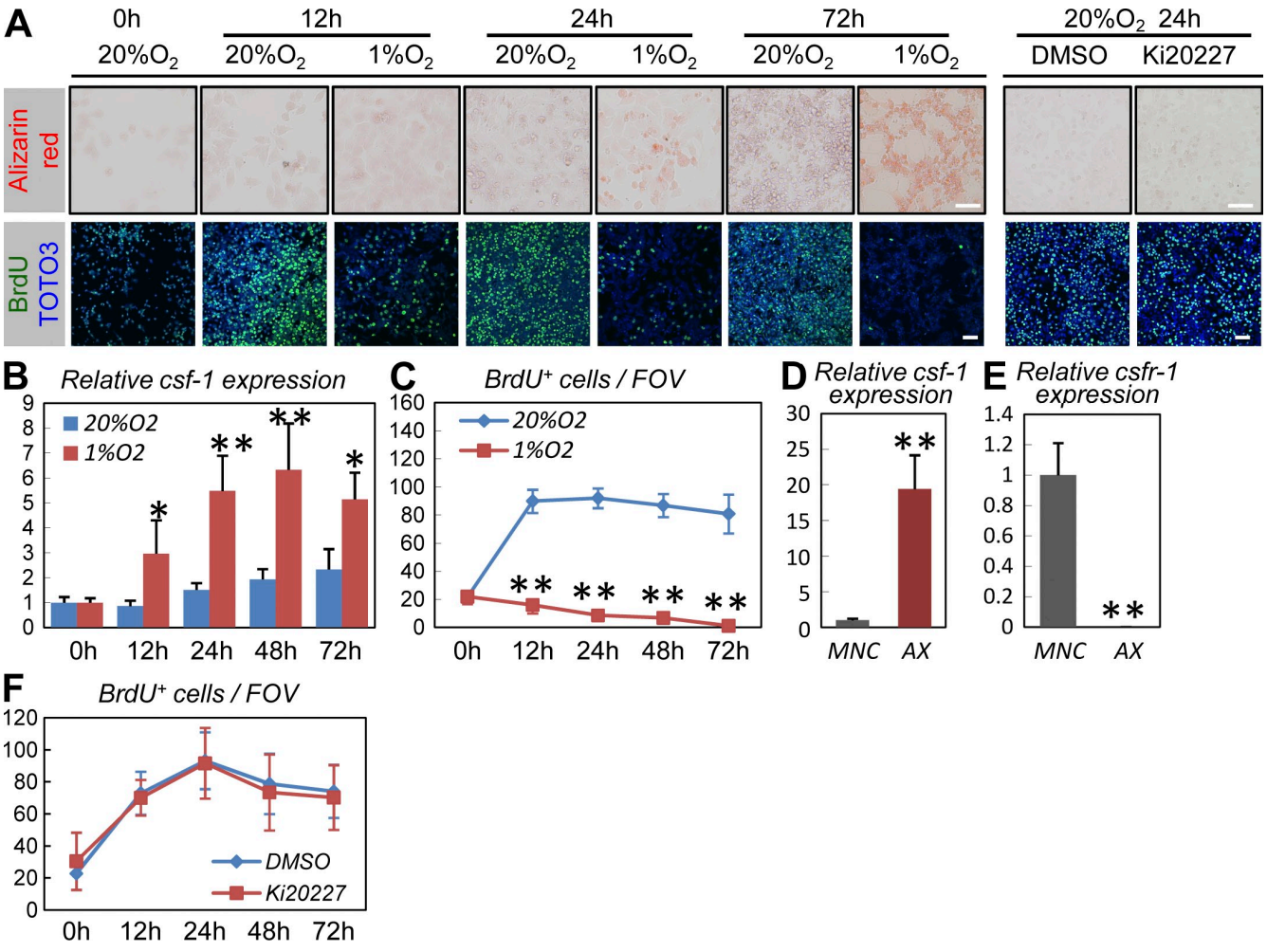

Figure S4. **Hypoxia, but not Ki20227, induces osteogenic differentiation and decreases proliferation in cultured AX cells.** (A) Representative images of Alizarin red staining (top) and IHC for BrdU (green; bottom) in AX cells grown in 20% O_2, 1% O_2, or AX cells supplemented with 100 nM Ki20227 dissolved in DMSO or vehicle only (representative images of five independent experiments). Note that hypoxic culture conditions, but not Ki20227, induced early calcification and decreased BrdU incorporation. (B) Relative expression (mean ± SD) of *csf-1* in AX cells at the indicated time points (n = 5; all experiments were performed in quadruplicate and the means for each sample were obtained). (C) Quantification (mean ± SD) of BrdU+ AX cells (n = 5). *, P < 0.03; **, P < 0.01 (compared with 20% O_2 at each time point). (D and E) Relative expression (mean ± SD) of *csf-1* (D) or *csfr-1* (E) in cultured MNCs on day 2 or in subconfluent AX cell cultures (n = 5). **, P < 0.01 (compared with MNC). (F) Quantification (mean ± SD) of BrdU+ AX cells (n = 5). Bars, 50 µm.

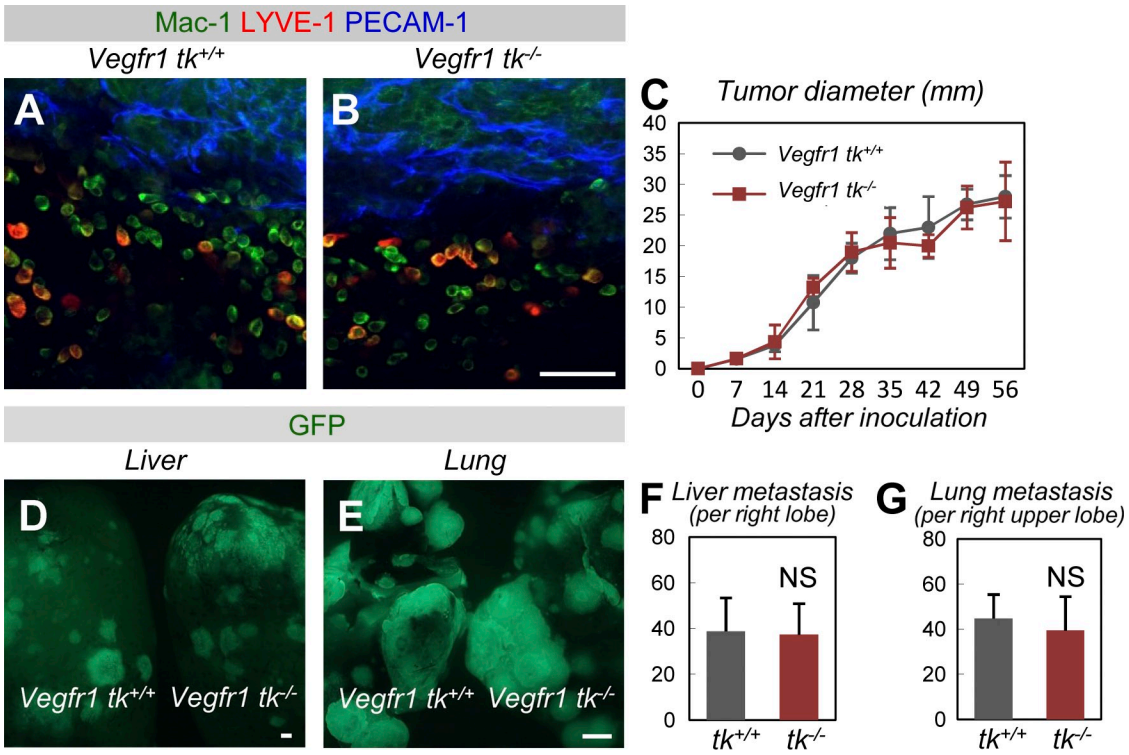

Figure S5. Macrophage recruitment in mouse osteosarcoma is less dependent on VEGF/Flt1 signaling. (A and B) An IHC analysis of Mac-1 (green), PECAM-1 (blue), and LYVE-1 (red) in tumors 21 d after transplantation (representative images of four independent experiments). Tumors in *Vegfr1 tk*$^{-/-}$ mice exhibited macrophage recruitment comparable to tumors in wild-type mice. (C) Quantification (mean ± SD) of tumor diameter (n = 4). (D and E) Fluorescent views in the liver (D) or lung (E) 56 d after tumor inoculation (representative images of four independent experiments). Note that the number of metastatic masses is not affected in *Vegfr1 tk*$^{-/-}$ mice. (F and G) Quantification (mean ± SD) of liver (F) or lung (G) metastasis at day 56 (n = 4). Bars: (B) 50 µm; (D and E) 200 µm.